IEEE Access
Multidisciplinary ⋮ Rapid Review ⋮ Open Access Journal

Received 4 February 2024, accepted 21 February 2024, date of publication 27 February 2024, date of current version 11 March 2024.

Digital Object Identifier 10.1109/ACCESS.2024.3370944

RESEARCH ARTICLE

On the Adaptive Modulation for User-Centric Cell-Free Massive MIMO Systems

DANILO B. T. ALMEIDA[1], MARCELO S. ALENCAR[1,2], (Life Senior Member, IEEE), RAFAEL M. DUARTE[3], HUGERLES S. SILVA[4,5], (Member, IEEE), FRANCISCO MADEIRO[6], WASLON T. A. LOPES[7], (Senior Member, IEEE), AND WAMBERTO J. L. QUEIROZ[1]

[1]Department of Electrical Engineering, Federal University of Campina Grande (UFCG), Campina Grande, Paraíba 58429-900, Brazil
[2]Department of Communications Engineering, Federal University of Rio Grande do Norte, Natal, Rio Grande do Norte 59078-900, Brazil
[3]Department of Computer Engineering, Federal University of São Francisco Valley (Univasf), Juazeiro, Bahia 48902-300, Brazil
[4]Departamento de Eletrónica, Telecomunicações e Informática, Instituto de Telecomunicações, Universidade de Aveiro, Campus Universitário de Santiago, 3810-193 Aveiro, Portugal
[5]Department of Electrical Engineering, University of Brasília (UnB), Brasília, Federal District 70910-900, Brazil
[6]Polytechnic School of Pernambuco, University of Pernambuco (UPE), Recife, Pernambuco 50720-001, Brazil
[7]Department of Electrical Engineering, Federal University of Paraíba (UFPB), João Pessoa, Paraíba 58059-970, Brazil

Corresponding author: Waslon T. A. Lopes (waslon@ieee.org)

This work was supported in part by Brazilian Coordination for the Improvement of Higher Education Personnel (CAPES)—Finance Code 001, in part by the National Council for Scientific and Technological Development (CNPq) under Grant 309286/2022-0, and in part by the Foundation for Science and Technology (FCT)/Portuguese Ministry of Science, Technology, and Higher Education (MCTES) through National Funds and co-funded by European Union (EU) Funds under Project UIDB/50008/2020-UIDP/50008/2020.

ABSTRACT The cell-free (CF) systems are a key technology for future wireless networks, which exploit the scenario spatial macro-diversity to offer high channel capacity and link reliability, uniform user quality of service (QoS), and better coverage. A technique for access point selection (APS) must be applied to improve the use of the macro-diversity. This paper proposes a low-complexity APS technique based on the derived signal-to-interference-plus-noise ratio (SINR) theoretical expression. Additionally, to increase the system's spectral efficiency (SE), an expression for the bit error probability (BEP) of the generic square M_m-ary quadrature amplitude modulation (M_m-QAM) scheme for each user is proposed and applied to an adaptive modulation (AM) algorithm. The results revealed that the proposed APS technique outperforms techniques with similar simplicity and that the AM algorithm provides higher system SE maintaining the error rate below a given threshold.

INDEX TERMS Access point selection, adaptive modulation, bit error probability, cell-free, spectral efficiency.

I. INTRODUCTION

The cell-free massive multiple-input multiple-output (mMIMO) concept has emerged as an attractive alternative to address future system demands and it is considered for the realization of sixth-generation networks [1]. Different from traditional cellular architecture, cell-free (CF) systems assume a boundary-free coverage area in which a large number of distributed access points (AP) are placed to serve all the user equipment (UE) simultaneously. By applying the distributed antennas concept, the CF systems can take advantage of the spatial macro-diversity to exhibit high levels of spectral efficiency (SE) and uniformity of user quality of service (QoS) [2].

When first presented, the cell-free concept assumed that each UE was served by all available AP [2], [3], [4], [5]. However, further investigations revealed that selecting subsets of APs to serve UEs, a methodology known as user-centric (UC) approach (or device-centric) [6], can improve the system's performance [7], [8], [9]. Indeed, in some situations, the AP to UE channel attenuation may be severe enough to drop the signal power below the receiver sensibility, so that only noise would be delivered by the AP to the UE. Additionally, if close enough UEs are served by the same AP, high interference levels may be experienced by each other. Thus, a proper technique to assign APs to UEs must be applied to improve the system performance by decreasing the

The associate editor coordinating the review of this manuscript and approving it for publication was Stefan Schwarz.

multiuser interference [8], [10], [11], [12], [13], [14], [15], [16], [17], [18], [19].

In this paper, we propose to group the access point selection (APS) into two classes: slow and fast. The slow AP to UE assignment performs APS within the time in which the large-scale fading (LSF) remains constant, which is assumed to vary slowly compared to the small-scale fading (SSF). In this strategy, the APS focuses on maximizing, for example, the average system SE, but may fail to attain it if the channel varies suddenly [13], [14], [15], [16], [17], [18], [19]. In the fast APS, the AP to UE assignment is performed on the SSF coherence time, so, whenever it varies, the system must be able to adjust the selected APs for each UE [8], [10], [11], [12]. This strategy focuses on the maximization of the instantaneous system performance but demands higher system processing. As in slow APS, the assignment is performed on the LSF coherence time, the computational cost decreases, sometimes at the expense of rate gains. In this context, several works analyzed different ways to perform AP selection to increase the system performance [8], [13], [14], [16], [18], [19].

A. LITERATURE REVIEW

In one of the first works to compare the UC approach concept with CF, the authors considered that the system used the estimated instantaneous channel coefficients to perform APS, and then, analyzed the saving guaranteed by the UC approach, in terms of required backhaul capacity [8]. In the mentioned work, the APS methodology selects a set of access points whose link exhibits the highest estimated channel coefficients to define a virtual cell for each UE. Additionally, although lower required backhaul, one could not observe the UC gains, in terms of downlink per UE rate, leading the authors to state that an adaptive APS methodology would be enough to provide a better system performance. Several works used a similar AP to UE assignment strategy to analyze different aspects of the new UC approach. The first comparison of the UC and the conventional CF at millimeter waves was presented in [10]. Two methodologies were presented in [11] for power control aiming either the maximization of the UE sum rates or the minimum UE rates, guaranteeing UE QoS fairness, and an extended version, considering both the APs and UEs equipped with multiple antennas, was presented in [12].

The aforementioned works performed fast APS based on the instantaneous estimated channel coefficients. Although this strategy tracks the channel variations more precisely, it demands higher backhaul capacity and central processing unit (CPU) overload. Hence, some works proposed slow APS based on the channel LSF coefficient. For example, an APS was proposed in [13] using the average channel power, which is equal to the LSF coefficient, coupled with power control optimization. The authors focused on UE QoS fairness and analyzed the impact of increasing the size of the virtual cell by increasing the number of selected APs per UE.

The recent findings proving the superiority of the UC approach when compared to conventional CF, not only in terms of less required backhaul capacity but also in terms of SE, requested the APS methodologies to be more relevant and sophisticated. An adaptive pilot assignment algorithm was proposed in [14] based on the UE virtual cell, making use of the LSF coefficient. The algorithnm first performs APs clusterization, then ensures that the UEs with fewer commonly selected APs share the same pilot sequence, to decrease the pilot contamination and increase the system per UE rates. The authors demonstrated that the proposed combined APS with pilot assignment outperforms the random pilot assignment technique.

Due to the slow varying LSF characteristics, the slow AP to UE assignment attracted several authors owing to the system performance improvement at the cost of low computational effort. A simple APS rule based on the LSF coefficient was considered in [16] to analyze a CF operating in an indoor factory environment, making use of different precoders to prove the superiority of the UC approach. In turn, a similar APS technique was performed to analyze the channel aging effects due to the UE mobility, then a dynamic AP to UE assignment technique was proposed in [15] to decrease the unnecessary number of handovers caused by the channel variations.

The congestion game theory was applied to perform an APS technique based on two principles, selecting the least number of UEs connected to the same AP, to reduce the selected AP fronthaul requirement, and selecting the APs with the highest relative LSF coefficient, as one can see in [17]. According to the authors, the proposed APS technique was able to highly decrease the required fronthaul for each selected AP, but could not adjust adequately the per-user data rate. Alternatively, a CF system was treated as a multi-agent reinforcement learning (MARL) system to address the APS problem, as one can see in [18]. First of all, the clustering was modeled as a Markov game in which each state was based on the received signal strength (RSS), which is proportional to the LSF, and then two policies were adopted: the maximization of the SE sum and the maximization of the minimum SE, demonstrating that the MARL-based algorithm was able to increase the maximum SE sum by 87.6% of the conventional CF.

A two-layer APS algorithm with different strategies for fine-tuning was proposed in [19], either decreasing the number of UEs per AP, without decreasing the system SE or maintaining the energy efficiency (EE). In the first layer, each UE connects to an intermediate AP based on the LSF coefficient, preventing the signal from dropping, and in the second layer, each UE expands its cluster by connecting to more APs to increase the SE. The authors found that the proposed method was able to increase the 95%-likely SE up to 163%.

After applying an optimization technique, such as selecting the set of APs, or adjusting the per UE transmitted power, that provides the higher system sum rates or uniformizes

UEs QoS, it is worthing analyzing the system performance in terms of any metric to verify the gains introduced by the optimization technique. Recent works addressed the analysis of the CF performance in terms of the number of bit or symbol errors [20], [21], [22], [23]. For instance, two different receivers were proposed in [20], one based on the expectation propagation (EP) algorithm, and another based on the generalized least square (GLS) technique, to reduce receiver complexity. The results were presented in terms of the bit error rate (BER), analyzing how CF suffers the influence of the system fronthaul capacity and average signal-to-noise ratio (SNR). Later on, the authors presented an analysis of the optimum AP to UE antenna distribution. Although the authors presented new receiver structures to overcome classical receivers, the results were presented using the simulated BER, instead of the theoretical bit error probability (BEP). However, the simulated results are not practical to perform real-time optimization.

Theoretical BEP bounds for CF systems were presented in [21]. The authors derived a new distributed EP receiver, and then presented new BEP expressions by assuming that the received signal could be expressed as an additive white Gaussian noise (AWGN) channel, by uncoupling the signal to the SSF. The new distributed EP receiver was proposed to circumvent the high computational overhead demanded by classical receivers. However, it is not clear how the SSF effects were taken into account and how the multiuser interference was treated.

A different framework, considering cloud-based CF systems, was applied in [23] to derive a symbol error probability (SEP) theoretical expression. The authors derived the pairwise error probability and then extended the results to obtain the asymptotic SEP expression. Afterwards, the authors proposed two different types of detectors to overcome the interference, inspired by the successive interference cancellation (SIC) technique. The SEP bounds were analyzed for different system configurations. Finally, the authors stated that deriving a theoretical BEP expression would be extremely difficult due to the number of erroneous events it would incorporate.

B. CONTRIBUTIONS

In the present paper, an expression is derived for the CF UE average signal-to-interference-plus-noise ratio (SINR), making use of Lyapunov's central limit theorem (LCLT) to approximate the multiuser interference to a complex Gaussian random variable and incorporating the randomness introduced by the SSF. The expression is applied to perform slow APS using a simple methodology that aims to increase each UE average SINR, which differs from of the fast APS proposed in [8], [10], [11], and [12], to secure low backhaul capacity requirement. Furthermore, differently from the works that used the LSF to perform slow APS [13], [14], [15], [16], [17], [18], [19], the usage of the SINR for AP to UE assignment incorporates information about three different characteristics simultaneously: the interference, the noise, and the signal powers. Thus, the proposed APS may present an improved behavior for real scenarios.

To analyze the proposed APS performance, a new UE BEP expression is derived, and an adaptive modulation (AM) technique is applied. The derived expression makes use of the known LSF coefficients to compute each UE BEP, taking into account the SSF characteristics, by averaging the BEP of the generic M_m-QAM scheme for AWGN channel by the SSF distribution. The AM algorithm is applied to increase the channel usage and the system average SE.

In summary, the main contributions of this paper are:

- *Proposition of an APS technique*: a new and simple APS technique is proposed to assign APs and UEs to maximize each UE average SINR. The AP to UE assignment is performed on the LSF coherence time, aiming to increase the average SE, while decreasing backhaul load;
- *Derivation of a UE BEP expression*: a new closed-form expression is derived for each UE BEP, considering the knowledge of the LSF coefficients and taking into account the SSF characteristics. Similarly to the APS methodology, the BEP values given by the expressions are valid whenever the LSF coefficients remain constant, allowing the usage of the APS methodology combined with an AM technique;
- *Combined APS and AM optimization*: both the APS and AM techniques, using the derived BEP expressions, are applied to increase the system average SE.

C. PAPER OUTLINE AND NOTATIONS

The next sections of the paper are organized as follows. In Section II, the system model is presented and the choice of SSF and LSF is justified. The instantaneous and mean SINR and BEP expressions are derived in Section III, and in Section IV, the APS and AM techniques are presented. The results obtained after the application of the APS and AM techniques are presented in Section V. The final considerations, conclusion, and future works are presented in Section VI.

Notation: Lowercase letters denote random variables and the superscript $(\cdot)^*$ denotes the complex conjugate. The expectation operador and the complex Gaussian random variable x are denoted, respectively, by $E[\cdot]$ and $\mathcal{CN}(\mu_x, \sigma_x^2)$, in which both the mean and the variance of x are μ_x and σ_x^2, respectively.

II. SYSTEM MODEL

To model both the CF and the UC systems, a coverage area of $D \times D$ m^2 is considered, in which K UEs and M APs are randomly positioned according to a uniform distribution. Between each pair of UE and AP, there is a link with a different channel. It is considered that all the M APs are connected to the same central processing unit (CPU) and the system operates according to a time division duplex (TDD) protocol, in which the frames are divided into three portions:

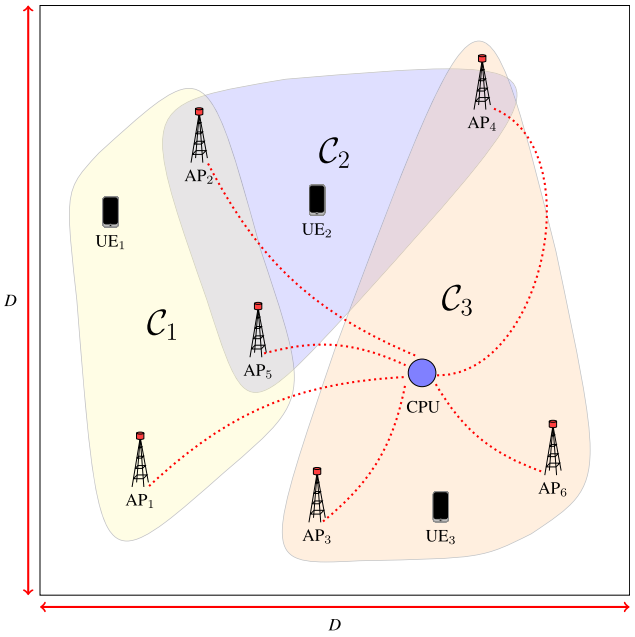

FIGURE 1. Representation of a cell-free system.

channel estimation, downlink payload data transmission, and uplink payload data transmission. [2]. For the UC approach, it is assumed that, according to the channel conditions, S APs are chosen within the M available ones to serve the k-th EU, composing the cluster $\mathcal{C}_k$, as shown in Fig. 1.

The channel gains reciprocity are assumed throughout the downlink and uplink (payload and training) phases. The channel coefficient is composed of both the LSF effect, characterized using the log-normal distribution for the shadowing and the alpha-beta-gamma (ABG) path loss distributions, and the slow flat SSF effect, characterized using the uncorrelated Rayleigh model. Unlike the SSF coefficient, which is considered to remain constant for a coherence time interval of τ_s symbols, the large-scale fading coefficients vary more slowly and may be considered constant for multiple transmitted frames, or τ_l, so it can be assumed to be perfectly estimated [3].

The channel gain between the k-th UE and the m-th AP, g_{mk}, is given by [3]

$$g_{mk} = \beta_{mk}^{1/2} h_{mk}, \tag{1}$$

in which β_{mk} and h_{mk} are the large and small-scale fading coefficients, respectively. Additionally, it is assumed that the distance between pairs of APs and UEs is large enough that a pair of coefficients h_{mk} and β_{mk} is considered independent of another pair $h_{m'k'}$ and $\beta_{m'k'}$, $\forall$ $\{m, k\}$ different from $\{m', k'\}$. Consequently, no spatial correlation in shadowing is considered here.

In downlink payload transmission mode, the pre-coded signal transmitted by the m-th AP, containing the data addressed to all K UEs, is given by [2]

$$x_m = \sqrt{\rho_d} \sum_{k=1}^{K} \eta_{mk}^{1/2} \hat{g}_{mk}^{*} q_k, \tag{2}$$

in which ρ_d is the downlink transmitted power and $\hat{g}_{mk}^{*}$ is the complex conjugate of the estimated channel gain. Furthermore, the power control coefficient is denoted by η_{mk} and q_k is the data transmitted symbol with power σ_q^2. The values of η_{mk}, for uniform power control, may be given by [4]

$$\eta_{mk} = \left(\sum_{i=1}^{K} \beta_{mi} \right)^{-1}, \tag{3}$$

so that $\|x_m\|^2 = \rho_d \sigma_q^2$.

In this research, it is intended to apply AM and APS to improve the system SE. So, without loss of generality, uniform power control is considered.

In the downlink transmission, the received signal at the k-th UE is given by

$$r_k = \sum_{m=1}^{M} g_{mk} x_m + w_k \tag{4}$$

$$= \sqrt{\rho_d} \sum_{m=1}^{M} \sum_{k'=1}^{K} \eta_{mk'}^{1/2} g_{mk} \hat{g}_{mk'}^{*} q_{k'} + w_k \tag{5}$$

$$= \alpha_k q_k + \psi_k + w_k \tag{6}$$

in which w_k is the complex AWGN at the k-th receiver, α_k is what we call effective channel gain, written as

$$\alpha_k = \sqrt{\rho_d} \sum_{m=1}^{M} \eta_{mk}^{1/2} g_{mk} \hat{g}_{mk}^{*}, \tag{7}$$

and ψ_k is the multiuser interference experienced by the k-th UE as a result of the signal transmitted by the APs to the other $K-1$ UEs in the system, given by

$$\psi_k = \sqrt{\rho_d} \sum_{m=1}^{M} \sum_{\substack{j=1 \\ j \neq k}}^{K} \eta_{mj}^{1/2} g_{mk} \hat{g}_{mj}^{*} q_j. \tag{8}$$

In the current work, it is assumed perfect channel state information (CSI), so that $\hat{g}_{mk} = g_{mk}$. This consideration allows the sum in (7) to be characterized using the generalized chi-square (GCS) distribution with PDF given by [24]

$$p_{\alpha_k}(x) = \sum_{m=1}^{M} \frac{\exp\left(-\frac{x}{\sigma_{mk}}\right)}{\sigma_{mk} \prod_{j=1, j \neq m}^{M} \left(1 - \frac{\sigma_{jk}}{\sigma_{mk}}\right)} u(x), \tag{9}$$

in which $u(x)$ represents the unit step function and $\sigma_{mk} = \eta_{mk}^{1/2} \rho_d^{1/2} \beta_{mk}$ is the per link fading standard deviation.

Also, by applying the LCLT [25], the multiuser interference ψ_k can be approximated so that $\psi_k \sim \mathcal{CN}(0, \sigma_{\psi_k}^2)$, in which

$$\sigma_{\psi_k}^2 = \sum_{m=1}^{M} \sum_{\substack{j=1 \\ j \neq k}}^{K} \rho_d \eta_{mj} \beta_{mk} \beta_{mj} \sigma_q^2. \tag{10}$$

Making use of the knowledge about the distributions of α_k, ψ_k and w_k, one can find the user instantaneous SINR PDF and derive the BEP for each UE.

III. INSTANTANEOUS SINR AND BEP OF THE K-TH UE

This work focuses on the analysis of average statistics given the prior knowledge of the LSF coefficients β_{mk}, but taking into account the randomness introduced by the effective SSF α_{mk}. This approach allows the systems to make use of optimization techniques with decision-making in the LSF variation time, reducing computational efforts, for example. With this aim, the SINR concept, and the derived BEP, must hold for each LSF coherence time τ_l.

A. INSTANTANEOUS SINR OF THE K-TH UE

Given the *a priori* knowledge of β_{mk}, the instantaneous SINR at the output of the k-th UE receiver can be written as

$$\gamma_k = \alpha_k^2 \frac{E\left[|q_k|^2\right]}{E\left[|\psi_k + w_k|^2\right]} = \alpha_k^2 \gamma_{qk}, \tag{11}$$

in which $E[\cdot]$ is the expected value operator and

$$\gamma_{qk} = \frac{\sigma_q^2}{2\left(\sigma_{\psi_k}^2 + \sigma_w^2\right)}. \tag{12}$$

Furthermore, using (9), one can show that the instantaneous SINR of the k-th UE has its values distributed according a PDF given by

$$p_{\gamma_k}(y) = \sum_{m=1}^{M} \frac{y^{-\frac{1}{2}} \exp\left(-\frac{\sqrt{y}}{\sigma_{mk}\sqrt{\gamma_{qk}}}\right)}{2\sigma_{mk}\sqrt{\gamma_{qk}} \prod_{j=1, j\neq m}^{M}\left(1 - \frac{\sigma_{jk}}{\sigma_{mk}}\right)} u(y), \tag{13}$$

whose mean value is

$$\bar{\gamma}_k = \sum_{m=1}^{M} \frac{2\gamma_{qk}\sigma_{mk}^2}{\prod_{j=1, j\neq m}^{M}\left(1 - \frac{\sigma_{jk}}{\sigma_{mk}}\right)}. \tag{14}$$

The PDF of the SINR may be used to derive different metrics, such as BEP, channel capacity, outage probability and the average theoretical SINR to perform AP clusterization.

B. BEP OF THE K-TH UE

Assuming that the channel gain remains constant along the τ_s interval, the knowledge of β_{mk} must be enough for deriving the BEP of the k-th UE, denoted by P_k. Therefore, if the BEP of the M_m-QAM, assuming AWGN channel and gray mapping, can be expressed by [27]

$$P_k = \frac{1}{\log_2\sqrt{M_m}} \sum_{j=1}^{\log_2\sqrt{M_m}} P_k(j), \tag{15}$$

in which $P_k(j)$ is the error probability in the j-th bit, one can take into account the random nature of the effective channel gain α_k, to write

$$P_k(j) = \int_0^{\infty} P_k(j|\gamma_k) p_{\gamma_k}(\gamma_k) d\gamma_k, \tag{16}$$

in which

$$P_k(j|\gamma_k) = \frac{1}{\sqrt{M_m}} \sum_{i=0}^{(1-2^{-j})\sqrt{M_m}-1} \zeta_{ij} \operatorname{erfc}\left(\sqrt{\frac{a_i \gamma_k}{\log_2 M_m}}\right), \tag{17}$$

with

$$a_i = \frac{3(2i+1)^2 \log_2 M_m}{2(M_m - 1)}, \tag{18}$$

$$\zeta_{ij} = (-1)^{\left\lfloor \frac{i2^{j-1}}{\sqrt{M_m}} \right\rfloor} \left(2^{j-1} - \left\lfloor \frac{i2^{j-1}}{\sqrt{M_m}} + \frac{1}{2} \right\rfloor\right), \tag{19}$$

$\lfloor\cdot\rfloor$ denoting the floor function and $\operatorname{erfc}(\cdot)$ the complementary error functions.

One can show that

$$P_k(j) = \frac{2}{\pi\sqrt{M_m}} \sum_{i=0}^{(1-2^{-j})\sqrt{M_m}-1} \zeta_{ij} f_i(\gamma_{b_k}), \tag{20}$$

in which

$$\begin{aligned} f_i(\gamma_{b_k}) &= \int_0^{\frac{\pi}{2}} \int_0^{\infty} \exp\left(-\frac{\gamma_k}{\log_2 M_m} \frac{a_i}{\sin^2\theta}\right) p_{\gamma_k}(\gamma_k) d\gamma_k d\theta \\ &= \int_0^{\frac{\pi}{2}} M_{\gamma_k}\left(-j\frac{a_i}{\log_2 M_m \sin^2\theta}\right) d\theta, \end{aligned} \tag{21}$$

with $M_{\gamma_k}(\omega)$ denoting the moment generation function of γ_k, given by

$$M_{\gamma_k}(\omega) = \frac{\sqrt{\pi}}{2} \sum_{m=1}^{M} \frac{\operatorname{erfc}\left(\frac{1}{2\sqrt{j\sigma_{mk}^2\gamma_{q_k}\omega}}\right) \exp\left(\frac{1}{j4\sigma_{mk}^2\gamma_{q_k}\omega}\right)}{\sqrt{j\sigma_{mk}^2\gamma_{q_k}\omega} \prod_{j=1, j\neq m}^{M}\left(1 - \frac{\sigma_{jk}}{\sigma_{mk}}\right)}. \tag{22}$$

Additionally, using the fact that [26]

$$\exp(z)\operatorname{erfc}\left(\sqrt{z}\right) = \frac{1}{\pi} G_{1,2}^{2,1}\left[z\middle|\begin{matrix}\frac{1}{2} \\ 0, \quad \frac{1}{2}\end{matrix}\right] \tag{23}$$

and making the substitution $v(\theta) = \sin\theta$, one can show that

$$\begin{aligned} f_i(\gamma_{b_k}) = \frac{1}{2} \sum_{m=1}^{M} & \frac{1}{\prod_{j=1, j\neq m}^{M}\left(1 - \frac{\sigma_{jk}}{\sigma_{mk}}\right)} \\ & \times G_{2,3}^{2,2}\left[\frac{1}{4\sigma_{mk}^2\gamma_{b_k}a_i}\middle|\begin{matrix}1, & \frac{1}{2} \\ \frac{1}{2}, & 1, \quad 0\end{matrix}\right], \end{aligned} \tag{24}$$

with

$$\gamma_{b_k} = \frac{1}{\log_2 M_m} \gamma_{q_k} \tag{25}$$

denoting the k-th UE per bit SINR, and $G_{2,3}^{2,2}[\cdot|\cdot]$ the Meijer-G function [28].

It is worth mentioning that, given the values of β_{mk}, the system average BEP $\bar{P}$ is written as

$$\bar{P} = \frac{1}{K}\sum_{k=1}^{K} P_k. \tag{26}$$

Using P_k, one can apply AM technique. Besides that, $\bar{P}$ may be used to evaluate the system performance.

IV. ACCESS POINT SELECTION AND ADAPTIVE MODULATION TECHNIQUES

After the acquisition of the values of β_{mk}, the system must make decisions like calculating the power control coefficient η_{mk} of links between each pair of AP and UE, performing the selection of the proper constellation order of M_m-QAM and defining the methodology for AP to UE association. It is worth mentioning that derived metrics must be valid for τ_l long intervals, and the system must make decisions accordingly. This section focuses on the presentation of techniques for AM and AP to UE association according to the UC approach.

A. ACCESS POINT AND USER EQUIPMENT ASSOCIATION TECHNIQUE

In this work, two different AP to UE association rules are compared: the first one is based on the LSF coefficients β_{mk} and the other is inspired on (14). For the β_{mk} based technique, referred to as APS [16], the CPU sorts the acquired β_{mk} for each UE and selects the S APs whose AP to UE links present the highest β_{mk} [16].

For the SINR-based methodology, referred to as Proposed APS, the strategy that provides the highest performance is the one that aims to maximize all $\bar{\gamma}_k$ simultaneously. However, as the search space for the S selected APs for all the K UE grows fast with S, M, and K, this strategy leads to high computational effort. Therefore, to save processing time, the proposed technique takes into account each AP to UE link SINR $\bar{\gamma}_{mk}$ instead. Thus, for each UE, the CPU calculates and sorts the values of the SINR of each link, given by

$$\bar{\gamma}_{mk} = \frac{\sigma_q^2 \sigma_{mk}^2}{\sigma_w^2 + \sigma_{\psi_{mk}}^2}, \tag{27}$$

in which $\sigma_{\psi_{mk}}^2 = \sum_{\substack{j=1 \\ j\neq k}}^{K} \rho_d \eta_{mj} \beta_{mk} \beta_{mj} \sigma_q^2$, and selects the S APs whose AP to UE links present the best SINR, as depicted in Fig. 2. It is worth mentioning that, although Proposed APS technique does not find the highest possible $\bar{\gamma}_k$ for all UE simultaneously, it guarantees a higher $\bar{\gamma}_k$ per UE when compared to APS [16].

It is worth mentioning that the APS using the LSF coefficient may not be the best choice because, although higher β_{mk} indicates lower attenuation levels, no further insights are given into how this entity is related to the other channel characteristics, such as noise power σ_w^2 and user experienced interference power $\sigma_{\psi_k}^2$. Indeed, if the k-th UE selects one AP due to its high β_{mk} value, but that AP transmits enough interfering signals, it may contribute to a decrease in the observed $\bar{\gamma}_k$ and lower the system performance. Thus, Proposed APS can exploit the system characteristics in a better manner with similar complexity presented in APS [16].

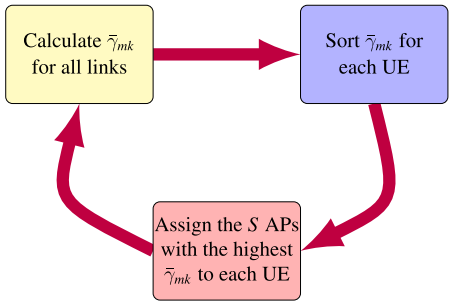

FIGURE 2. Proposed APS chart.

B. ADAPTIVE MODULATION ALGORITHM

This work considers a discrete order AM technique based on P_k to increase the average SE maintaining the observed BEP below a certain threshold. To achieve this goal, the CPU makes use of the acquired β_{mk} and the results calculated using (15) to properly select the modulation order. The decisions made must be updated whenever the LSF coefficient varies.

For each UE, the AM technique first calculates the P_k for different orders of square M_m-QAM scheme, using (15), and choose the higher M_m order which gives $P_k < T_{tsh}$, in which T_{tsh} is the desired threshold BER [29], [30]. Once the CPU defines the scheme order of each UE, the APs selected using the presented APS techniques transmit the data symbols to its assigned UEs using the selected M_m-QAM schemes for a τ_l long interval.

If one defines π_{M_m} as the occurrence probability of the M_m-QAM scheme, the average SE may be given by [30]

$$C = \sum_{M_m} \pi_{M_m} \log_2 M_m. \tag{28}$$

The average SE is used to analyze the gains given by the application of the APS rules coupled with the applied AM technique.

V. RESULTS

In the simulations, each scenario realization comprises a region of $D \times D$ m^2, with $D = 650$ m, in which M APs and K UEs are randomly positioned, according to a two-dimensional uniform distribution, and assuming that $\tau_l = 40$ frames of $\tau_c = 200$ symbols are transmitted. The path loss parameters characterize a system operating at the central frequency of 28 GHz, considering an urban macro cell with no line-of-sight, or NLoS [31]. The results concern the AM presented technique considering that the system can make use of 4-QAM, 16-QAM and 64-QAM, and both the APS rules. Finally, to extract enough statistics, $N_R = 500$ scenario realizations are performed.

Curves of P_k as a function of $\bar{\gamma}_k$ are shown in Fig. 3. Exclusively for this result, a single channel realization was

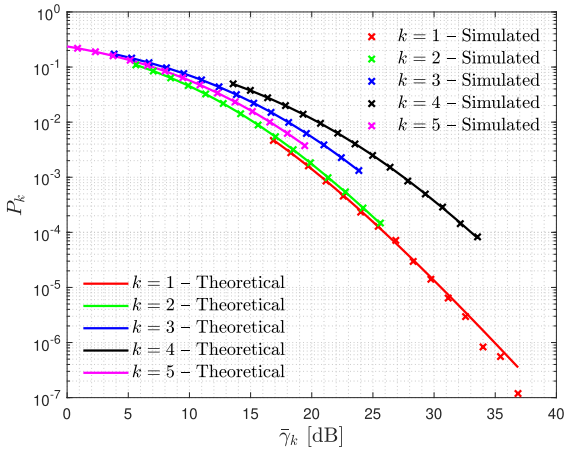

(a) Curves of BEP and BER as a function of the SINR considering the 4-QAM modulation.

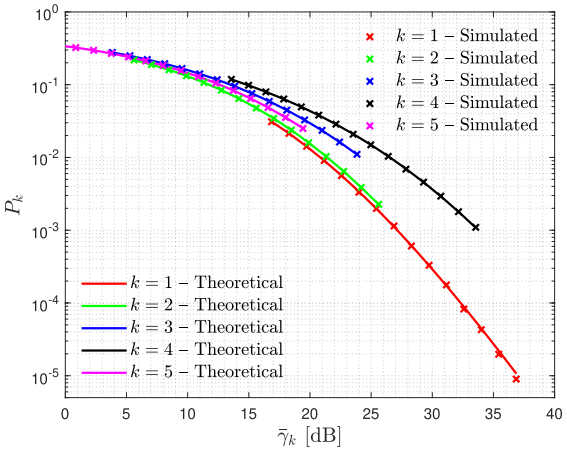

(b) Curves of BEP and BER as a function of the SINR considering the 16-QAM modulation.

FIGURE 3. Curves of P_k for different UEs, considering $M = 50$ APs, $K = 5$ UEs, $S = 5$ selected APs using the proposed APS technique as a function of each UE mean experienced SINR.

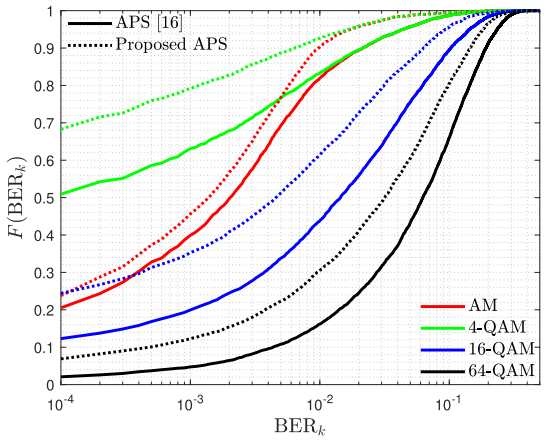

FIGURE 4. Curves of the eCDF the per UE BER for different modulation schemes, considering $\rho_d = 0.48$ W, $M = 100$ APs, $K = 10$ UEs, $S = 10$ selected APs and $T_{tsh} = 10^{-2}$.

performed in which the $K = 5$ UEs and the $M = 50$ APs positions are obtained randomly, but kept fixed together with the shadowing coefficients. Additionally, to obtain suficient statistics, the number of frames sent, while the UEs and the APs positions and the shadowing coefficients are not changed, is increased to $\tau_l = 10^6$. Furthemore, ρ_d was varied in the range of 10 mW to 1 W.

Note that, in Fig. 3, the UEs experience different $\bar{\gamma}_k$ ranges and this happens due to the LSF coefficients. Looking at (2), it is evident that, after the precoding and the multiplication by η_{mk}, a residual effect of the β_{mk} is still affecting the sent information, which, in some situations, is enough to decrease $\bar{\gamma}_k$, as one can see, for example, with the UEs $k = 2$ and $k = 4$. Furthermore, even on UEs with similar $\bar{\gamma}_k$ ranges, P_k may vary due to the effects of the SSF. Indeed, although all UEs downlink SSF are characterized using the GCS distribution with S degrees of freedom, the parameters that determine the distribution shape may differ from UE to UE, leading different UEs to present different P_k, even at the same $\bar{\gamma}_k$ value, as one can observe on UEs $k = 2$, $k = 3$ and $k = 5$ at 15 dB. Additionally, from Fig. 3, it is worth mentioning that the system may benefit from an optimized power control coefficient to grant QoS fairness and uniformize, for instance, P_k.

Curves are shown in Fig. 4 for the empirical cumulative density function (eCDF) of the per UE BER, considering N_R scenario realizations, for $T_{tsh} = 10^{-2}$. It can be observed that the proposed SINR-based APS technique is more likely to offer lower per UE BER for all analyzed modulation schemes. Additionally, regarding the AM, one can verify that, for $P_k > T_{tsh}$, the eCDFs curves tend to follow the 4-QAM ones, but decrease and get closer to the high modulation orders curves for $P_k < T_{tsh}$. For situations in which the channel conditions do not allow a BER below the threshold, the algorithm forces the usage of the 4-QAM scheme. However, as long as the channels conditions improve, higher-order modulations are expected to be selected by the AM algorithm, increasing the average SE at the cost of increasing P_k, but maintaining it below T_{tsh}.

In Fig. 5, curves are shown for the average system BER and π_{M_m} as a function of ρ_d for different modulation schemes. From Fig. 5(a), it can be verified that the average system BER decreases, but exhibits a saturation trend as ρ_d grows. This saturation occurs due to the rising interference power $\sigma^2_{\psi_k}$ as ρ_d increases, which causes the SINR to become approximately constant because $\sigma^2_{\psi_k} \gg \sigma^2_w$. In Fig. 5(b), it is possible to notice that as ρ_d increases, higher-order modulations are more likely to be selected by the AM technique for both APS methodologies. From Fig. 5, one can state that Proposed APS provides better system performance as it allows the system to operate in a lower BER regime selecting high-order modulations more often. For example,

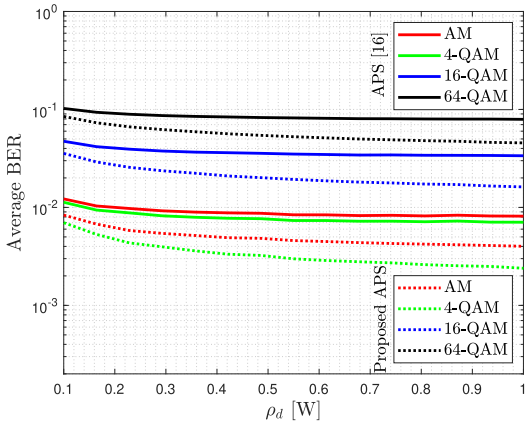

(a) Average system BER for different modulation schemes as a function of ρ_d.

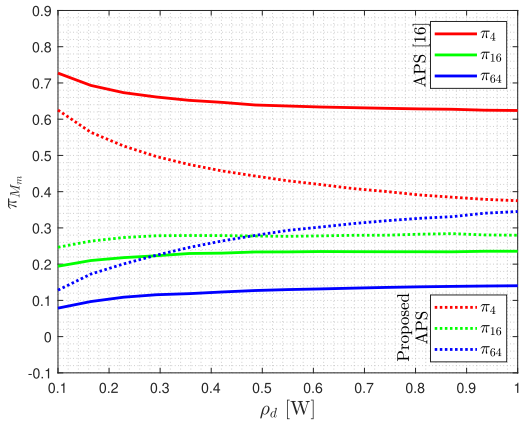

(b) Occurrence probability π_{M_m} for different modulation schemes as a function of ρ_d.

FIGURE 5. Average system BER and occurrence probabilities as a function of ρ_d considering $M = 100$ APs, $K = 10$ UEs, $S = 10$ selected APs and $T_{tsh} = 10^{-2}$.

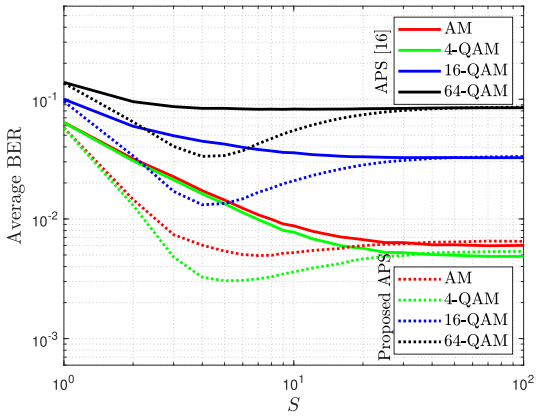

(a) Average system BER for different modulation schemes as a function of S.

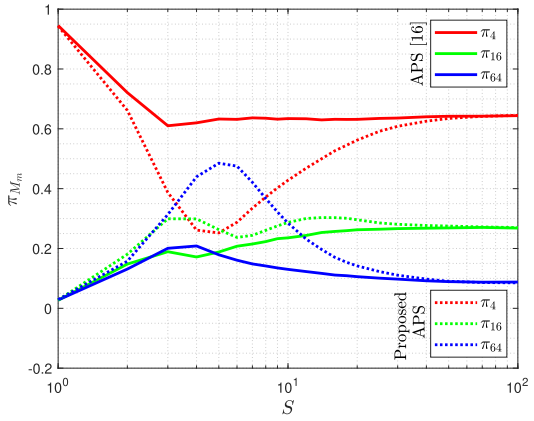

(b) Occurrence probability π_{M_m} for different modulation schemes as a function of S.

FIGURE 6. Average system BER and occurrence probabilities as a function of ρ_d considering $M = 100$ APs, $K = 10$ UEs, $\rho_d = 0.5$ W and $T_{tsh} = 10^{-2}$.

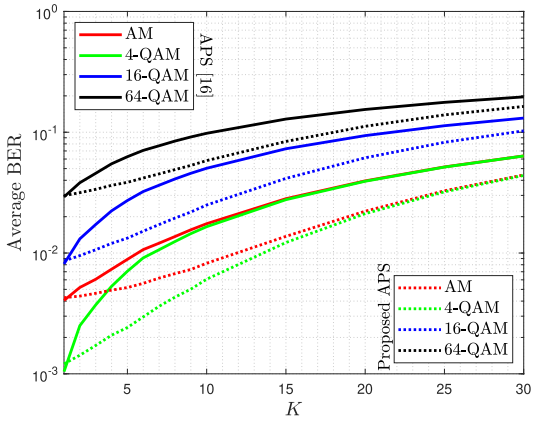

(a) Average system BER for different modulation schemes as a function of K.

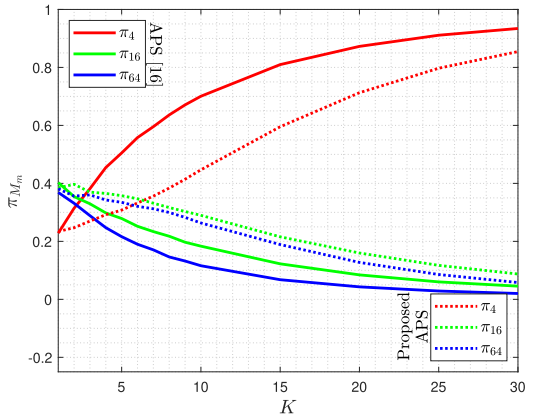

(b) Occurrence probability π_{M_m} for different modulation schemes as a function of K.

FIGURE 7. Average system BER and occurrence probabilities as a function of K considering $M = 100$ APs, S=5 selected APs, $\rho_d = 0.2$ W and $T_{tsh} = 10^{-2}$.

for $\rho_d = 0.5$ W and using APS [16] rule, the AM technique selects the 64-QAM with probability equal to 12%, but with probability 28% if the proposed APS technique is applied, leading to a higher data rate.

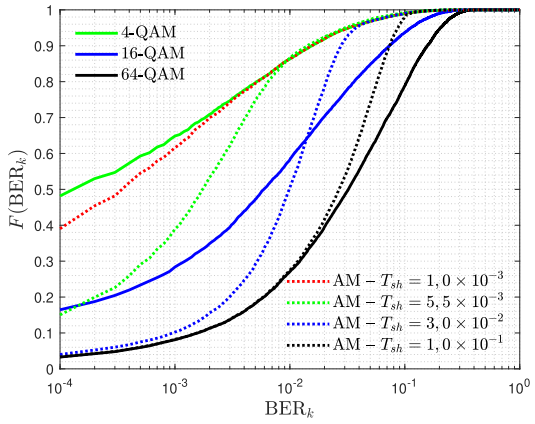

(a) Empirical CDF of the UE BER for different values of T_{tsh} and different modulation schemes, using Proposed APS.

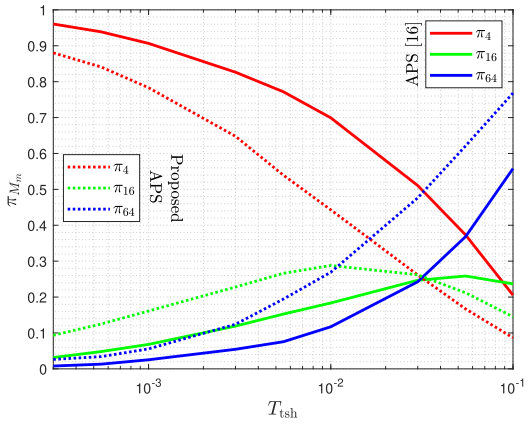

(b) Occurrence probability π_{M_c} for different values of T_{tsh} as a function of K.

FIGURE 8. Empirical CDF of the UE BER and occurrence probabilities as a function of T_{tsh} considering $M = 100$ APs, $K = 10$ UEs, $S = 5$ selected APs and $\rho_d = 0.2$ W.

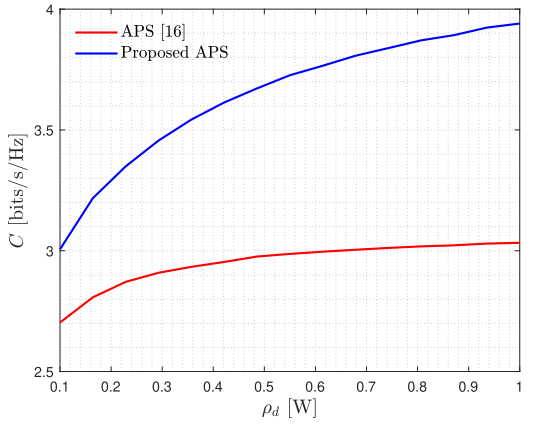

(a) Curves of C considering $M = 100$ APs, $K = 10$ UEs, $S = 10$ selected APs and $T_{\mathrm{tsh}} = 10^{-2}$ as a function of ρ_d.

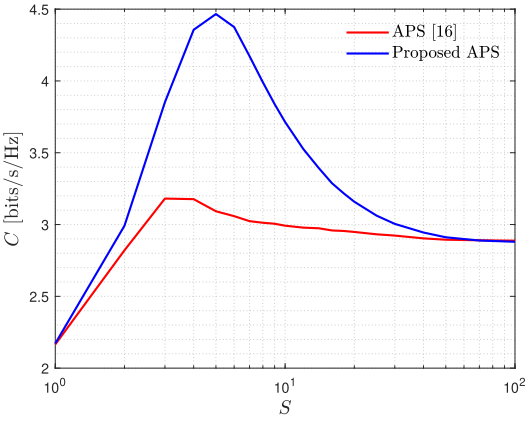

(b) Curves of C considering $M = 100$ APs, $K = 10$ UEs, $\rho_d = 0.5$ W and $T_{\mathrm{tsh}} = 10^{-2}$ as a function of S.

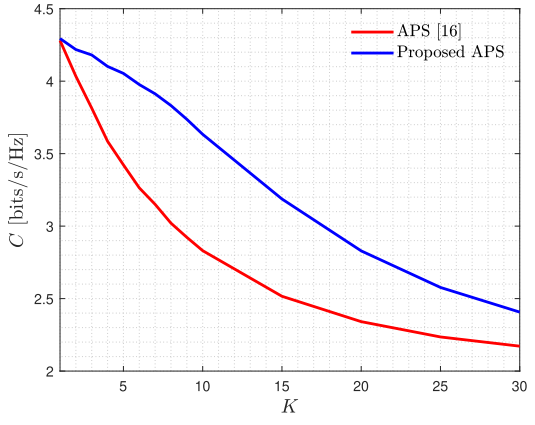

(c) Curves of C considering $M = 100$ APs, $\rho_d = 0.2$ W, $S = 5$ selected APs and $T_{\mathrm{tsh}} = 10^{-2}$ as a function of K.

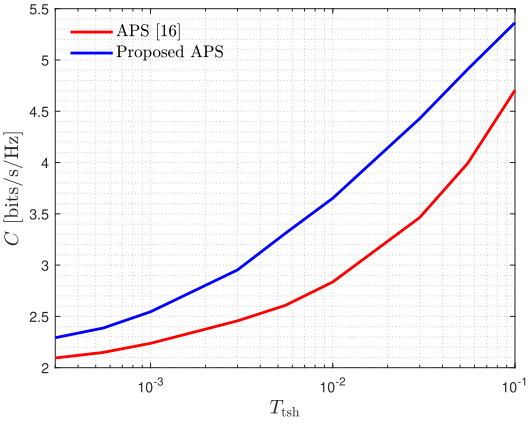

(d) Curves of C considering $M = 100$ APs, $K = 10$ UEs, $\rho_d = 0.2$ W and $S = 5$ selected APs as a function of T_{tsh}.

FIGURE 9. Curves of C for $M = 100$ for the AM technique assuming both Proposed APS and APS [16] for AP selection.

Curves of the average system BER and π_{M_m} as a function of S, for different modulation schemes, can be observed in Fig. 6. As one can see in Fig. 6(a), the use of the proposed APS allows the system to reach a lower average system BER when compared to APS [16], for all considered modulation schemes. For instance, using the SINR-based technique, the minimum average system BER for the AM scheme is 5×10^{-3} for $S = 7$, but is 6×10^{-3} for $S = 70$ using

the β_{mk}-based rule. Furthermore, in Fig. 6(b), one observes that the maximum system average SE occurs for $S < 10$ for both APS techniques and so, Proposed APS can provide a lower average system BER operating at the maximum average SE region, differently from APS [16]. Additionally, one should notice that as S increases both APS rules present similar average BER and π_{M_m}, and this happens because the probability of both techniques selecting the same APs grows with S. Besides that, for lower values of S, the proposed APS allows the AM technique to select the 16-QAM and 64-QAM modulation more often, increasing the average SE.

The effect of increasing the number of attended UE on the average system BER and on the π_{M_m} for a CF system operating under different APS rules and using the described AM technique is presented in the Fig. 7. From Fig. 7(a), it can be verified that increasing K has a negative effect on the system performance, and this occurs due to the increasing $\sigma^2_{\psi_k}$ with K and because the power control coefficients are inversely proportional to K, thus decreasing the per UE received energy as K increases, the consequence of which is the limitation of $\bar{\gamma}_k$. Regarding the APS techniques, one can see that higher-order modulations are more likely to be selected by the AM algorithm and that the average BER growth rate is lower for the proposed APS and this may be explained by the fact that APS [16] does not take into account the relation of the channel strength indicator β_{mk} with the increasing $\sigma^2_{\psi_k}$, differently from Proposed APS that aims to increase $\bar{\gamma}_k$ regardless of the level of the interference.

In Fig. 8, the effects of varying T_{tsh} in π_{M_m} are observed. It is clear that, although higher values of T_{tsh} increase the probability of high order modulations, it forces the UEs to experience higher BER more often. For instance, considering the proposed APS, for T_{tsh} increasing from 5.5×10^{-3} to 3×10^{-2}, the probability of the occurrence of the 64-QAM goes from 20% to 48%, but the probability of the UEs to experience BER below 1×10^{-2} decreases from 85% to 48%. Furthermore, in Fig. 8(b), one can see that using the APS rule proposed in this work, the AM technique is more likely to select higher order modulations for all analyzed values T_{tsh}, increasing the system average SE.

An analysis of C can be carried out using Fig. 9. One should notice that, for all analyzed scenarios, the results obtained using the AM and the proposed APS techniques behave as a performance upper bound when compared to the β_{mk}-based APS technique. For instance, in addition to the higher C level, its curve saturation is not evident for the analyzed ρ_d range when the AM technique is allied to the proposed SINR-based APS, as shown in Fig. 9(a). Furthermore, looking at Fig. 9(b), one can see that although APS [16] reaches the maximum $C = 3.18$ bits/s/Hz for a lower number of selected APs $S = 3$, what leads to a lower CPU effort, the maximum system average SE is 40.40% higher when Proposed APS is applied, reaching $C = 4.47$ bits/s/Hz for a slightly increasing in the number of selected APs, or $S = 7$. Additionally, revisiting Fig. 6, one should remember that the maximum C occurs at a higher BER regime when the β_{mk}-based APS technique is applied, but close to the minimum BER regime for the proposed one. Analyzing Fig. 9(c), although C decreases as K grows, due to the higher levels $\sigma^2_{\psi_k}$, when Proposed APS is used, the system can take advantage of the links that provide higher $\bar{\gamma}_{mk}$ to increase the average SE, what leads to a slower decreasing C as K grows, when compared to the use of APS [16]. Finally, as one can see in Fig. 9(d), higher levels of average SE is verified as T_{tsh} increases because the AM technique selects higher order modulations. However, selecting higher order modulation schemes demands the application of robust error corrector codes due to the system higher error level.

VI. CONCLUSION

In this paper, a novel expression for the per EU BEP for CF systems was derived and a simple technique for APS was proposed, based on the theoretical per UE SINR. The new BEP expression was used for an AM technique application to improve the system SE. A comparison of the BER and SE results was carried out for both APS techniques. The results demonstrated that, in addition to the higher level of system average SE attained, the proposed APS technique allowed the system to operate closer to the maximum achievable average SE at a lower BER regime, and that the increasing number of UE does not degrade the average SE as fast as the APS found in the literature. The use of the per-link SINR to perform APS incorporates three channel characteristics, the average signal power, the interference power, and the noise power, which revealed the SINR to be a better metric, over the LSF coefficient, for APS purposes, and that the proposed APS technique outperforms the LSF-based one demanding a similar amount of system resources.

DATA AVAILABILITY

The data used to support the findings of this study are available from the corresponding author upon request.

DECLARATION OF COMPETING INTEREST

The authors declare that there is no conflict of interest regarding the publication of this paper.

REFERENCES

[1] A. Shahraki, M. Abbasi, M. Jalil Piran, and A. Taherkordi, "A comprehensive survey on 6G networks: Applications, core services, enabling technologies, and future challenges," 2021, *arXiv:2101.12475*.

[2] H. Q. Ngo, A. Ashikhmin, H. Yang, E. G. Larsson, and T. L. Marzetta, "Cell-free massive MIMO: Uniformly great service for everyone," in *Proc. IEEE 16th Int. Workshop Signal Process. Adv. Wireless Commun. (SPAWC)*, Jun. 2015, pp. 201–205.

[3] H. Q. Ngo, A. Ashikhmin, H. Yang, E. G. Larsson, and T. L. Marzetta, "Cell-free massive MIMO versus small cells," *IEEE Trans. Wireless Commun.*, vol. 16, no. 3, pp. 1834–1850, Mar. 2017.

[4] E. Nayebi, A. Ashikhmin, T. L. Marzetta, and H. Yang, "Cell-free massive MIMO systems," in *Proc. 49th Asilomar Conf. Signals, Syst. Comput.*, Nov. 2015, pp. 695–699.

[5] E. Nayebi, A. Ashikhmin, T. L. Marzetta, and B. D. Rao, "Performance of cell-free massive MIMO systems with MMSE and LSFD receivers," in *Proc. 50th Asilomar Conf. Signals, Syst. Comput.*, Nov. 2016, pp. 203–207.

[6] P. Fiati, "5G: New air interface and radio access virtualization," Huawei Technol. Co. Ltd., Shenzhen, China, White Paper, Apr. 2015. [Online]. Available: https://www-file.huawei.com/minisite/media/tech-whiter-paper/pdf/hw_424967.pdf

[7] L. Wang and Q. Liang, "Optimization for user centric massive MIMO cell free networks via large system analysis," in *Proc. IEEE Global Commun. Conf. (GLOBECOM)*. IEEE, 2016, pp. 1–6.
[8] S. Buzzi and C. D'Andrea, "Cell-free massive MIMO: User-centric approach," *IEEE Wireless Commun. Lett.*, vol. 6, no. 6, pp. 706–709, Dec. 2017.
[9] S. Buzzi, C. D'Andrea, and C. D'Elia, "User-centric cell-free massive MIMO with interference cancellation and local ZF downlink precoding," in *Proc. 15th Int. Symp. Wireless Commun. Syst. (ISWCS)*, Aug. 2018, pp. 1–5.
[10] M. Alonzo and S. Buzzi, "Cell-free and user-centric massive MIMO at millimeter wave frequencies," in *Proc. IEEE 28th Annu. Int. Symp. Pers., Indoor, Mobile Radio Commun. (PIMRC)*, Oct. 2017, pp. 1–5.
[11] S. Buzzi and A. Zappone, "Downlink power control in user-centric and cell-free massive MIMO wireless networks," in *Proc. IEEE 28th Annu. Int. Symp. Pers., Indoor, Mobile Radio Commun. (PIMRC)*, Oct. 2017, pp. 1–6.
[12] S. Buzzi, C. D'Andrea, A. Zappone, and C. D'Elia, "User-centric 5G cellular networks: Resource allocation and comparison with the cell-free massive MIMO approach," *IEEE Trans. Wireless Commun.*, vol. 19, no. 2, pp. 1250–1264, Feb. 2020.
[13] Y. Li, Y. Zhang, and L. Yang, "Power control strategy for user-centric in cell-free massive MIMO," in *Proc. IEEE Int. Conf. Consum. Electron.*, May 2019, pp. 1–2.
[14] M. Sarker and A. O. Fapojuwo, "Granting massive access by adaptive pilot assignment scheme for scalable cell-free massive MIMO systems," in *Proc. IEEE 93rd Veh. Technol. Conf. (VTC-Spring)*, Apr. 2021, pp. 1–5.
[15] C. D'Andrea, G. Interdonato, and S. Buzzi, "User-centric handover in mmWave cell-free massive MIMO with user mobility," in *Proc. 29th Eur. Signal Process. Conf. (EUSIPCO)*, Aug. 2021, pp. 1–5.
[16] M. Alonzo, P. Baracca, S. R. Khosravirad, and S. Buzzi, "Cell-free and user-centric massive MIMO architectures for reliable communications in indoor factory environments," *IEEE Open J. Commun. Soc.*, vol. 2, pp. 1390–1404, 2021.
[17] L. Liu, S. Wu, Q. Ye, and Y. Ma, "An AP selection strategy based on congestion game for user-centric cell-free massive MIMO," in *Proc. IEEE 33rd Annu. Int. Symp. Pers., Indoor Mobile Radio Commun. (PIMRC)*, Sep. 2022, pp. 1099–1104.
[18] B. Banerjee, R. C. Elliott, W. A. Krzymien, and H. Farmanbar, "Access point clustering in cell-free massive MIMO using multi-agent reinforcement learning," in *Proc. IEEE 33rd Annu. Int. Symp. Pers., Indoor Mobile Radio Commun. (PIMRC)*, Sep. 2022, pp. 1086–1092.
[19] M. Freitas, D. Souza, G. Borges, A. M. Cavalcante, D. B. da Costa, M. Marquezini, I. Almeida, R. Rodrigues, and J. C. W. A. Costa, "Matched-decision AP selection for user-centric cell-free massive MIMO networks," *IEEE Trans. Veh. Technol.*, vol. 72, no. 5, pp. 6375–6391, May 2023.
[20] K. Ando, H. Iimori, T. Takahashi, K. Ishibashi, and G. T. F. De Abreu, "Uplink signal detection for scalable cell-free massive MIMO systems with robustness to rate-limited fronthaul," *IEEE Access*, vol. 9, pp. 102770–102782, 2021.
[21] H. He, H. Wang, X. Yu, J. Zhang, S. H. Song, and K. B. Letaief, "Distributed expectation propagation detection for cell-free massive MIMO," in *Proc. IEEE Global Commun. Conf. (GLOBECOM)*, Dec. 2021, pp. 1–6.
[22] J.-C. Guo, Q.-Y. Yu, W.-B. Sun, and W.-X. Meng, "Robust efficient hybrid pre-coding scheme for mmWave cell-free and user-centric massive MIMO communications," *IEEE Trans. Wireless Commun.*, vol. 20, no. 12, pp. 8006–8022, Dec. 2021.
[23] Y. Zhang, L. Xiao, and T. Jiang, "Cloud-based cell-free massive MIMO systems: Uplink error probability analysis and near-optimal detector design," *IEEE Trans. Commun.*, vol. 70, no. 2, pp. 797–809, Feb. 2022.
[24] E. Bjornson, D. Hammarwall, and B. Ottersten, "Exploiting quantized channel norm feedback through conditional statistics in arbitrarily correlated MIMO systems," *IEEE Trans. Signal Process.*, vol. 57, no. 10, pp. 4027–4041, Oct. 2009.
[25] P. Billingsley, *Probability and Measure*, 3rd ed. Hoboken, NJ, USA: Wiley, 1995.
[26] Wolfram Research. (2020). *Wolfram Research*. Accessed: Feb. 23, 2023. [Online]. Available: http://functions.wolfram.com/06.27.26.0008.01
[27] K. Cho and D. Yoon, "On the general BER expression of one- and two-dimensional amplitude modulations," *IEEE Trans. Commun.*, vol. 50, no. 7, pp. 1074–1080, Jul. 2002.
[28] I. S. Gradshteyn and I. M. Ryzhik, *Table of Integrals, Series, and Products*, 7th ed. Cambridge, MA, USA: Academic Press, 2014.
[29] V. N. Q. Bao, T. T. Thanh, and T. Do-Hong, "Performance analysis of adaptive modulation for distributed switch-and-stay combining with single relay," *REV J. Electron. Commun.*, vol. 1, no. 1, pp. 45–52, Apr. 2011.
[30] M. L. Ammari and P. Fortier, "Performance analysis of adaptive modulation for precoded MIMO systems with a GMD zero-forcing transceiver," *Wireless Pers. Commun.*, vol. 77, no. 3, pp. 2075–2097, Aug. 2014.
[31] S. Sun, T. S. Rappaport, S. Rangan, T. A. Thomas, A. Ghosh, I. Z. Kovacs, I. Rodriguez, O. Koymen, A. Partyka, and J. Jarvelainen, "Propagation path loss models for 5G urban micro- and macro-cellular scenarios," in *Proc. IEEE 83rd Veh. Technol. Conf. (VTC Spring)*, May 2016, pp. 1–6.

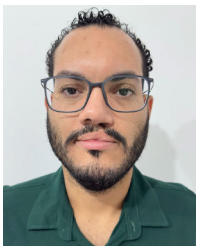

DANILO B. T. ALMEIDA was born in Itabaiana, Paraíba, Brazil, in 1989. He received the B.Sc. degree in electrical engineering from the University Federal of Campina Grande, Brazil, in 2016, where he is currently pursuing the D.Sc. degree. His research interests include channel modeling, estimation of parameters for wireless communication, and cell-free systems.

MARCELO S. ALENCAR (Life Senior Member, IEEE) received the bachelor's degree in electrical engineering from the Federal University of Pernambuco (UFPE), Brazil, the master's degree in electrical engineering from the Federal University of Paraíba (UFPB), Brazil, and the Ph.D. degree in electrical engineering from the University of Waterloo, Canada. He was with the Department of Electrical Engineering, UFPB; the Federal University of Campina Grande (UFCG); and the State University of Santa Catarina (UDESC). He was a Visiting Professor with the Federal University of Bahia (UFBA), Salvador, the Federal University of Rio Grande do Norte (UFRN), Brazil, and the University of Toronto, Canada. He has published over 550 engineering and scientific articles and 30 books. He has been awarded several scholarships and grants, from the Brazilian National Council for Scientific and Technological Research (CNPq), from the IEEE Foundation and from the University of Waterloo. He is a Laureate of the Prestigious 2014 Attilio Giarola Medal of the Brazilian Microwave and Optoelectronics Society (SBMO).

RAFAEL M. DUARTE received the bachelor's degree in electrical engineering and master's degree from the Federal University of Paraíba (UFPB), Brazil, in 2014 and 2016, respectively, and the Ph.D. degree from the Federal University of Campina Grande (UFCG) in May 2021. Throughout his academic life, he worked with electronic systems, signal processing and digital communications. Recently, he held the position of temporary teacher of basic and technical education (EBTT) at the Federal Institute of Mato Grosso (IFMT). In 2023, he returned to UFPB through a Post-Doctoral project in artificial intelligence. At the beginning of 2024, he took up the position of Professor at the Federal University of Vale do São Francisco (Univasf), where he began teaching electronics at the Dapartment of Computer Engineering (CEComp).

HUGERLES S. SILVA (Member, IEEE) received the B.Sc., M.Sc., and D.Sc. degrees in electrical engineering from the University Federal of Campina Grande, Brazil, in 2014, 2016, and 2019, respectively. He is currently an Adjunct Professor with the University of Brasília. His main research interests include wireless communication, digital signal processing, and wireless channel modeling.

FRANCISCO MADEIRO received the D.Sc. degree in electrical engineering from the Federal University of Paraiba (UFPB), Brazil, in 2001. Since 2006, he has been with the University of Pernambuco (UPE), Brazil, where he is currently an Associate Professor. He is also with the Catholic University of Pernambuco (UNICAP). His main research interests include signal processing, communications systems, computational intelligence, image encryption, and information hiding. He received the Distinguished Teaching Award for the year 2008 from the Polytechnic School of Pernambuco (POLI), UPE. He has contributed in Research and Development (R&D) and Research, Development and Innovation (RD&I) Projects. He received the Science and Technology Trophy, in the Outstanding Research and Outstanding Teaching categories from POLI/UPE, in 2013. He received the Science, Technology and Innovation Award, in the Outstanding Research Category from POLI/UPE, in 2018. He has published over 200 papers in journals and conference proceedings.

WASLON T. A. LOPES (Senior Member, IEEE) received the B.Sc. and M.Sc. degrees in electrical engineering from the Federal University of Paraíba (UFPB), Brazil, in 1998 and 1999, respectively, and the D.Sc. degree in electrical engineering from the Federal University of Campina Grande (UFCG), Brazil, in 2003. From November 2018 to October 2019, he was a Visiting Professor with the University of Toronto, Canada. Currently, he is an Associate Professor with the Department of Electrical Engineering, Center for Alternative and Renewable Energy, UFPB. He is the coauthor the books *Communications, Information and Network Security* (Kluwer Academic) and *Spectral Sensing: Techniques and Applications* (Momentum Press). His research interests includes robust vector quantization, wireless communication systems, communication theory, and digital signal processing.

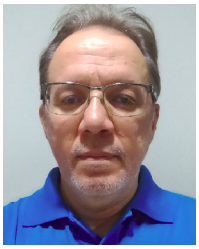

WAMBERTO J. L. QUEIROZ received the M.Sc. degree in electrical engineering from Federal University of Paraiba—UFPB, Campina Grande, Paraiba, in 2000, and the D.Sc. degree in electrical engineering from the Federal University of Campina Grande—UFCG, Campina Grande, in 2004. He was an Adjunct Professor with the Federal University of Ceará—UFC, from 2007 to 2010, joined UFCG, in 2010, where has been an Associate Professor, since 2018. His current research interests include digital communications over fading channels, channel modeling and simulations, spectrum sensing systems, and estimation theory.